



Kent Academic Repository

Howard, Mark J. and Rowe, Michelle L. (2013) *Structural Guided Scaffold Phage Display Libraries as a Source of Bio-Therapeutics*. *Structural Guided Scaffold Phage Display Libraries as a Source of Bio-Therapeutics*, 8 (n/a). e70452-e70452. ISSN 1932-6203.

Downloaded from

<https://kar.kent.ac.uk/35490/> The University of Kent's Academic Repository KAR

The version of record is available from

This document version

Publisher pdf

DOI for this version

Licence for this version

UNSPECIFIED

Additional information

Versions of research works

Versions of Record

If this version is the version of record, it is the same as the published version available on the publisher's web site. Cite as the published version.

Author Accepted Manuscripts

If this document is identified as the Author Accepted Manuscript it is the version after peer review but before type setting, copy editing or publisher branding. Cite as Surname, Initial. (Year) 'Title of article'. To be published in *Title of Journal*, Volume and issue numbers [peer-reviewed accepted version]. Available at: DOI or URL (Accessed: date).

Enquiries

If you have questions about this document contact ResearchSupport@kent.ac.uk. Please include the URL of the record in KAR. If you believe that your, or a third party's rights have been compromised through this document please see our [Take Down policy](https://www.kent.ac.uk/guides/kar-the-kent-academic-repository#policies) (available from <https://www.kent.ac.uk/guides/kar-the-kent-academic-repository#policies>).

Structural Guided Scaffold Phage Display Libraries as a Source of Bio-Therapeutics

Y. K. Stella Man¹✉, Danielle DiCara¹✉, Nicole Chan¹✉, Sandrine Vessillier², Stephen J. Mather³, Michelle L. Rowe⁴, Mark J. Howard⁴, John F. Marshall^{1*}, Ahuva Nissim^{2*}

1 Centre for Tumour Biology, Barts Cancer Institute, Queen Mary's University of London, London, United Kingdom, **2** Bone and Joint Research, William Harvey Research Institute, Queen Mary's University of London, London, United Kingdom, **3** Centre for Molecular Oncology and Imaging, Queen Mary's University of London, London, United Kingdom, **4** Biological NMR Spectroscopy, School of Biosciences, University of Kent, Canterbury, Kent, United Kingdom

Abstract

We have developed a structurally-guided scaffold phage display strategy for identification of ligand mimetic bio-therapeutics. As a proof of concept we used the ligand of integrin $\alpha\text{v}\beta\text{6}$, a tumour cell surface receptor and a major new target for imaging and therapy of many types of solid cancer. NMR structure analysis showed that RGD-helix structures are optimal for $\alpha\text{v}\beta\text{6}$ ligand-interaction, so we designed novel algorithms to generate human single chain fragment variable (scFv) libraries with synthetic $V_{\text{H}}\text{-CDR3}$ encoding RGD-helix hairpins with helices of differing pitch, length and amino acid composition. Study of the lead scFv clones D25scFv and D34scFv and their corresponding $V_{\text{H}}\text{-CDR3}$ derived peptides, D25p and D34p, demonstrated: specific binding to recombinant and cellular $\alpha\text{v}\beta\text{6}$; inhibition of $\alpha\text{v}\beta\text{6}$ -dependent cell and ligand adhesion, $\alpha\text{v}\beta\text{6}$ -dependent cell internalisation; and selective retention by $\alpha\text{v}\beta\text{6}$ -expressing, but not $\alpha\text{v}\beta\text{6}$ -negative, human xenografts. NMR analysis established that both the D25p and D34p retained RGD-helix structures confirming the success of the algorithm. In conclusion, scFv libraries can be engineered based on ligand structural motifs to increase the likelihood of developing powerful bio-therapeutics.

Citation: Man YKS, DiCara D, Chan N, Vessillier S, Mather SJ, et al. (2013) Structural Guided Scaffold Phage Display Libraries as a Source of Bio-Therapeutics. PLoS ONE 8(8): e70452. doi:10.1371/journal.pone.0070452

Editor: Zhaozhong Han, Vanderbilt University, United States of America

Received: March 30, 2013; **Accepted:** June 18, 2013; **Published:** August 9, 2013

Copyright: © 2013 Man et al. This is an open-access article distributed under the terms of the Creative Commons Attribution License, which permits unrestricted use, distribution, and reproduction in any medium, provided the original author and source are credited.

Funding: YKSM and NC were funded by the Dystrophic Epidermolysis Bullosa MARSHAL Research Association (<http://www.debra.org.uk/>). MJH is grateful for the award of Wellcome Trust (<http://www.wellcome.ac.uk>) Equipment Grant 091163/Z/10/Z for the NMR Spectrometer used in this project. The funders had no role in study design, data collection and analysis, decision to publish, or preparation of the manuscript.

Competing Interests: The authors have declared that no competing interests exist.

* E-mail: j.f.marshall@qmul.ac.uk (JM); a.nissim@qmul.ac.uk (AN)

✉ These authors contributed equally to this work.

Introduction

The use of combinatorial phage display scFv libraries for generation of therapeutic antibodies is well established and has resulted in clinically valuable reagents [1,2]. ScFv libraries are commonly made from immune or naïve B cells or as synthetic libraries where antibody variable heavy (V_{H}) and variable light (V_{L}) gene segments are rearranged *in vitro* with synthetic complementarity determining regions (CDRs) coding for random sequences of varying lengths [3–5]. The use of the phage display library has been used to develop antibodies for therapeutic intervention using the above combinatorial libraries. We reasoned that the use of antibody engineering in combination with ligand structural studies will result in robust libraries that can lead to isolation of potent ligand-mimetic bio-therapeutic antibody candidates.

Since receptor:ligand interactions must be considered as interacting topographical maps we wondered if it were possible to generate a target-selective library by incorporating a panel of specific three-dimensional shapes into the CDR3 of the variable heavy ($V_{\text{H}}\text{-CDR3}$). If such a library used stereochemical shapes that corresponded to a ligand-binding interface then it would more likely generate scFv(s) that will block the ligand:receptor interaction than would a conventional random library. To test this

hypothesis we considered a therapeutically relevant target, the integrin $\alpha\text{v}\beta\text{6}$, which represents a novel and important tumour-selective target that is expressed on the surface of cancer cells. We, and others, have shown that $\alpha\text{v}\beta\text{6}$ promotes cancer cell migration, invasion and growth *in vivo* [6–10]. Moreover strong expression of $\alpha\text{v}\beta\text{6}$ correlates with poor prognosis in multiple cancers [11–13] and thus human therapeutic antibodies to this integrin are likely to have a significant therapeutic value.

In previous studies we identified the 20mer peptide A20FMDV2 ($\text{N}_1\text{A}_2\text{V}_3\text{P}_4\text{N}_5\text{L}_6\text{R}_7\text{G}_8\text{D}_9\text{L}_{10}\text{Q}_{11}\text{V}_{12}\text{L}_{13}\text{A}_{14}\text{Q}_{15}\text{K}_{16}\text{-}_1\text{A}_2\text{V}_3\text{P}_4\text{N}_5\text{L}_6\text{R}_7\text{G}_8\text{D}_9\text{L}_{10}\text{Q}_{11}\text{V}_{12}\text{L}_{13}\text{A}_{14}\text{Q}_{15}\text{K}_{16}\text{V}_{17}\text{A}_{18}\text{R}_{19}\text{T}_{20}$), derived from the foot and mouth disease virus VP1 coat protein, as a highly specific and potent ligand for $\alpha\text{v}\beta\text{6}$ [14]. The peptide included the $\alpha\text{v}\beta\text{6}$ -binding motif RGD LXXL identified by Kraft et al (1999) [15]. Using NMR we determined the three-dimensional structure of A20FMDV2 in 30% TFE: a hairpin structure with RGD at the tip of the turn followed by a C-terminal helix [14]. This structural motif has also been observed in additional $\alpha\text{v}\beta\text{6}$ -binding peptides (Wagstaff et al, 2012, [14]). In addition, we have previously probed the role of the helix in A20FMDV2 through the use of specific D-amino acids to disrupt helix formation, and found the resulting helix-attenuated peptide had greatly reduced binding to cells expressing $\alpha\text{v}\beta\text{6}$ [14].

In this study we have used our NMR data to design algorithms to build phage display human scFv libraries that would retain the key structural residues that would encode a library of RGD-helix hairpin structural motifs where the helices could vary in length, pitch and sequence composition. Our data show that it is possible to design scFv libraries that include structural motifs within the V_H-CDR3 to provide potent ligand antagonising antibody candidates that can be developed for cancer therapy.

Results

Library design

Our rationale was to introduce a structural selectivity to a phage display library where the three-dimensional (3D) α v β 6 ligand recognition motif (RGD-helix) was genetically encoded into the antibody binding pocket at the V_H-CDR3. Figure 1A shows the amino-acid sequence identity and mean NMR solution structure of A20FMDV2. From these data plus the STD-NMR data [14] we designed two algorithms to develop V_H-CDR3 libraries encoding a hairpin containing at its turn, an RGD motif, followed by a C-terminal α -helix (Figure 1B) or a 3_{10} -helix (Figure 1C); the helical wheel map for each library is also shown. The template synthetic V_H-CDR3 was based on the α -helix donor sequence L₈A₉R₁₀L₁₁K₁₂R₁₃E₁₄F₁₅N₁₆E₁₇, which is helix 1 from the *Drosophila* engrailed homeodomain ((EN-HD) [16]). However in the library the L₈ was changed to A₈ in order to prevent formation of an LXXLL motif. The α -helix template V_H-CDR3 algorithm was: **E₁P₂R₃G₄D₅L₆X₇X₈L₉A₁₀A₁₁R₁₂Z₁₃K₁₄R₁₅Z₁₆F₁₇N₁₈E₁₉Z₂₀L₂₁A₂₂Z₂₃L₂₄Q₂₅E₂₆K₂₇G₂₈I₂₉** where **Z** and **X** were random amino-acid residues introduced into the same quadrant as the leucine residues of the RGD~~L~~XXLL motif: at position 13, 16, 20 and 23 in the α -helix based on the helical wheel (3.6 residues per turn of helix). The EP and the LQEKG~~I~~ motifs were N- and C-terminal helix-capping regions, respectively (based on the standard Schellmann C-cap: Leu-Gln-Glu-Lys-Gly-Ile (LQEKG~~I~~) [17] (Figure 1B). To extend the helix length further, the EN-HD donor sequence was repeated from positions 21/22 in the library. To build the 3_{10} helix library we used the E₁P₂R₃G₄D₅L₆X₇X₈L₉A₁₀A₁₁Z₁₂L₁₃K₁₄Z₁₅E₁₆F₁₇Z₁₈E₁₉N₂₀Z₂₁L₂₂A₂₃Z₂₄L₂₅Q₂₆E₂₇K₂₈G₂₉I₃₀ template inserting a random amino acid residue in every third position following the RGD~~L~~XXLL motif in the 3_{10} helix (3.0 residues per turn of 3_{10} helix, Figure 1C). Hence, the random residues automatically provided helices of different lengths because they included helix stabilising residues, such as alanine, lysine or arginine or, alternatively, helix destroying residues such as proline [18] as well as including residues covering all side chain properties to test the effect of charge, hydrophobicity and steric interactions.

Library selection and screening for lead candidates

After 3 rounds of alternate panning on immobilised recombinant α v β 6 and cells expressing α v β 6, greater than two thirds of clones bound to recombinant α v β 6 in ELISA (Figure 2A). Binders revealed at least 24 unique V_H-CDR3 sequences corresponding to both an α -helix and 3_{10} helix libraries. In flow cytometry experiments none of the scFv bound to the α v β 6-negative cells and many scFv bound well to the α v β 6-expressing cells. Since we used pair of cell lines that are isogenic and differ only by α v β 6 but endogenously express four other RGD directed integrins α 5 β 1, α v β 3, α v β 5 and α v β 8 [19,20] these data suggest strongly that the scFvs exhibited α v β 6-specific binding (Fig. 2B). However, based upon a combination of scFv protein expression yields, biochemical stability (size-exclusion chromatography) and strength of binding to cellular α v β 6 (flow cytometry) we focussed our study on 2

different scFvs clones: D25scFv (D25) and D34scFv (D34) (Figure 2C). V_H-CDR3 sequences of both D25 and D34 encoded α -helix as follows: **EPRGDLRTLAAREKRMFNETLARLQEKG~~I~~** and **QPRGDLRELAARSEAQLQEKG~~I~~**, for D25 and D34, respectively. Clone D34 had mutation from C to G that resulted in replacement of E to Q in the N-terminal helix-capping regions. The size-exclusion chromatography profile of the purified D34scFv showed a main peak eluting at 70 ml, corresponding to the 30 kDa scFv. For D25scFv we also observed a lower peaks eluting at 45–60 ml, corresponding to scFv dimers and tetramers, occasionally seen with some scFv [5] (Figure 2C).

α v β 6-specific antagonistic efficacy

A dose dependent binding analysis of both D25scFv and D34scFv and their corresponding V_H-CDR3 peptides (D25p and D34p, respectively) exhibited α v β 6-specific binding to A375P β 6 cells but not A375Ppuro (Figure 3A and Figure S1). Additionally, D25scFv, D34scFv, D25p and D34p showed a dose-dependent inhibition of binding to cellular α v β 6 of A20FMDV2 peptide (NAVPNLRGDLQVLAQKVART), a peptide that is 1000-fold more selective for α v β 6 over α 5 β 1, α v β 3, α v β 5 and α v β 8 integrins and binds with high affinity (K_D 1.7 nM) to the α v β 6 integrin [19] (Figure 3B–C). Moreover, D25scFv, D25p, D34scFv and D34p exhibited significant concentration-dependent inhibition of α v β 6-dependent adhesion of carcinoma cells to immobilised fibronectin (Figure 3D–E). Inhibition by D25p was significantly stronger than D34p ($p = 0.0156$)

α v β 6-specific internalization

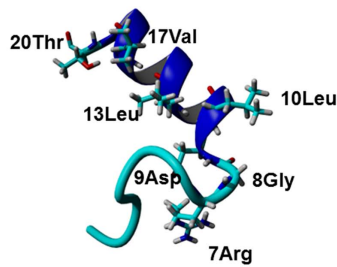
D25scFv and D34scFv exhibited cellular internalisation in α v β 6-expressing cells but not in α v β 6-negative cells. At 0 minutes, the scFvs were localised at the cell surface (Figure 4A and 4D for D25scFv and D34scFv, respectively) but after incubation at 37°C for 45 minutes, they were localised within the cell cytoplasm and nucleus (Figure 4B and 4E for D25scFv and D34scFv, respectively). Omitting the scFv primary layer and labelling only with anti-myc and the fluorochrome-labelled secondary antibody showed very little nuclear staining suggesting the nuclear localisation of the scFvs was real (Figure 4C and 4F for D25scFv and D34scFv, respectively). Similarly, biotinylated-D25p and biotinylated-D34p also underwent cellular internalisation in α v β 6-expressing cells (Figure 4H and 4K for D25p and D34p, respectively) but not in α v β 6-negative cells (Figure 4I, and 4L for D25p and D34p, respectively). Efficient internalisation was observed at 30–45 minutes (Figure 4H, K for D25p and D34p, respectively) but no nuclear localisation was observed.

Biotinylated-D25 peptide localises to α v β 6-expressing tumours *in vivo*

When 12.5MBq of [¹¹¹In]-DTPA-Streptavidin decorated with biotinylated-D25p was intravenously injected into three mice bearing both a subcutaneous α v β 6-positive A375P β 6 tumour and an α v β 6-negative A375Ppuro tumour, on opposite shoulders, we observed a 23% injected dose per gram uptake in the α v β 6-positive tumour compared with only 3% for the α v β 6-negative tumour at 1 hour post-injection, a ratio of almost 8:1 (Figure 5). This translated into a very clear discrimination of the α v β 6-positive tumour by single-photon emission computed tomography (SPECT) imaging (Figure 5).

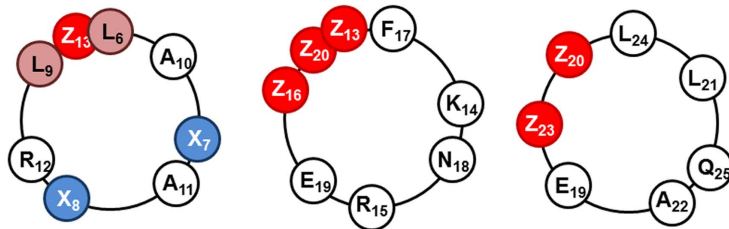
A. A20FMDV

N₁A₂V₃P₄N₅L₆R₇G₈D₉L₁₀Q₁₁V₁₂L₁₃A₁₄Q₁₅K₁₆V₁₇A₁₈R₁₉T₂₀



B. α helix:

E₁P₂R₃G₄D₅L₆X₇X₈L₉A₁₀A₁₁R₁₂Z₁₃K₁₄R₁₅Z₁₆F₁₇N₁₈E₁₉Z₂₀L₂₁A₂₂Z₂₃L₂₄Q₂₅E₂₆K₂₇G₂₈I₂₉



C. 3_{10} helix:

E₁P₂R₃G₄D₅L₆X₇X₈L₉A₁₀A₁₁Z₁₂L₁₃K₁₄Z₁₅E₁₆F₁₇Z₁₈E₁₉N₂₀Z₂₁L₂₂A₂₃Z₂₄L₂₅Q₂₆E₂₇K₂₈G₂₉I₃₀

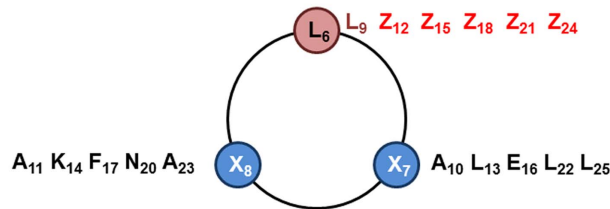


Figure 1. α -helix and 3_{10} -helix Library design. A) Amino acid sequence and NMR solution structure of A20FMDV2 with a hairpin structure with RGD at the tip of the turn followed by a C-terminal helix is shown. B) α -helix algorithm used to design the V_H-CDR3 encoding a hairpin containing at its turn an RGD motif, followed by a C-terminal α -helix. C) 3_{10} -helix algorithm used to design the V_H-CDR3 encoding a hairpin containing at its turn an RGD motif, followed by a C-terminal 3_{10} -helix. Amino acid positions that are available for randomisation are highlighted (X and Z shown in blue and red, respectively).

doi:10.1371/journal.pone.0070452.g001

Structural determination of D25 and D34 peptides by NMR

We used NMR to solve the solution structures for peptides D34p and D25p. Figure 6 shows the 3D-rendering model closest to the mean calculated for each peptide from an ensemble of 20 NMR structures; the associated structural statistical data from CNS for both peptides is available in Table S1 and NOE and structural contact information is available in Figures S2, S3, S4. Both peptides exhibited the RGD-helix motif. D34 which has 22 amino-acids has a shorter helix than peptide D25, which has 29 amino-acids. Helices for both peptides were defined as standard α -helix with the D34 α -helix running from Leu6-Leu17 and D25 α -helix running from Leu6-Gln25.

Discussion

CDR grafting, the replacing of complementarity-determining regions in a mouse antibody with those from a human antibody, has been used for more than two decades for humanization of

mouse monoclonal antibodies and development of immunotherapy [20]. CDR grafting of ligands into CDR loops to bind to a specific receptor was originally reported by Barbas *et al* in 1993 where they produced semisynthetic human antibodies library that included RGD motifs followed by random sequences to select for antibody fragments specific to the integrins $\alpha\beta 5$, $\alpha\beta 3$, and $\alpha_1\text{IIb}\beta 3$ [21]. Kogelberg *et al* inserted 17 residues from A20FMDV2 into the CDR3 region into an anti-CEA scFv thereby creating an antibody with $\alpha\beta 6$ -specificity [22]. More recently, a peptide sequence that bound to an inorganic material surface, was grafted into the CDR of a camel-type single domain antibody rearranged with a library of random sequences in additional CDR. Authors noted a synergistic effect from the grafted and selected random CDR loops that drastically increased the affinity for the inorganic target [23]. In this study we have taken a different approach, namely, grafting a 3-dimensional geometry based library designed from a ligand:receptor binding stereochemical interface. To test the model we chose a therapeutically valuable target, the integrin $\alpha\beta 6$ that we, and others, have

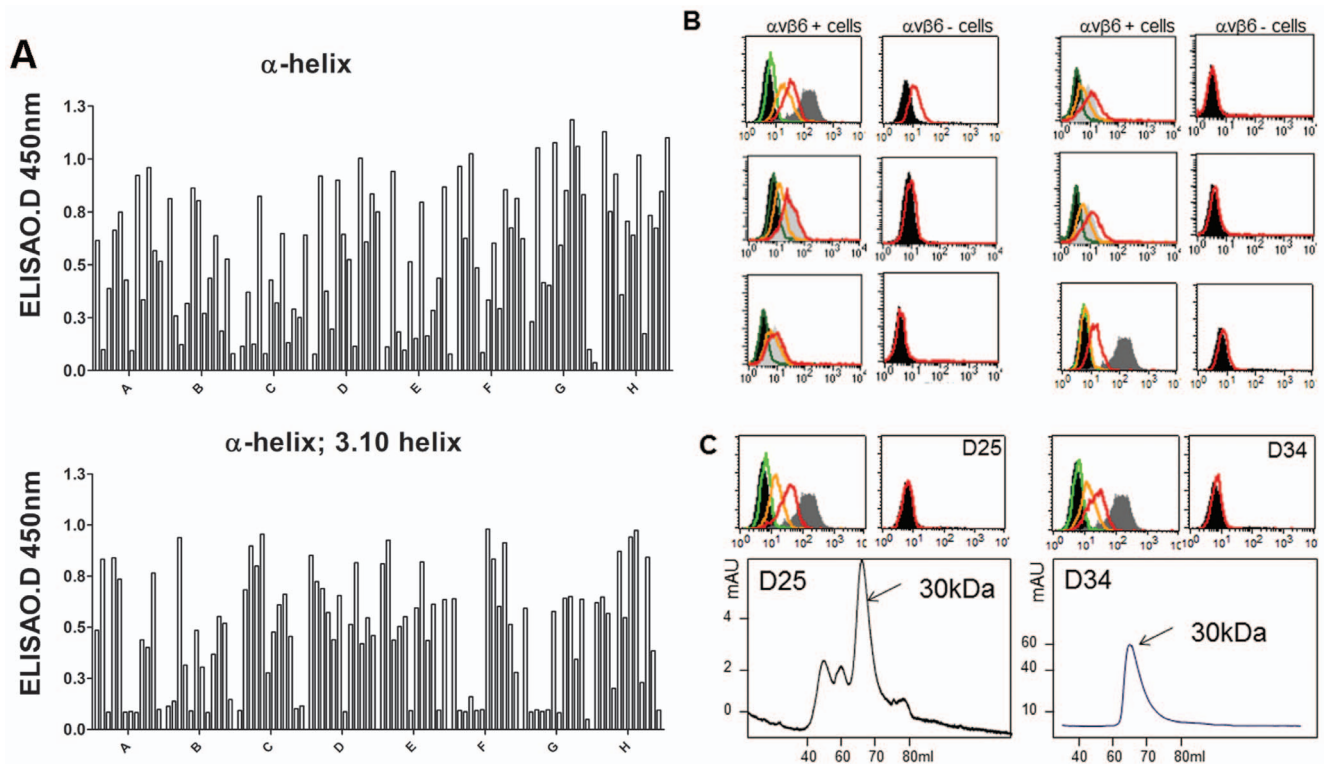


Figure 2. Screening of phage clones isolated from the α -helix & 3_{10} -helix libraries. A) Monoclonal scFv screening ELISA testing 96 clones in each library. Bacterial supernatants were added to 5 $\mu\text{g}/\text{ml}$ recombinant $\alpha\text{v}\beta 6$ immobilized onto ELISA plate and then probed with mouse anti-Myc antibody followed by anti-mouse-HRP. B) Clones with unique sequences were screened for binding cellular $\alpha\text{v}\beta 6$ by flow cytometry. Figure shows examples where scFv was tested at 100 (red histogram), 10 (orange histogram) and 1 (green histogram) $\mu\text{g}/\text{ml}$. For clarity the relevant $\alpha\text{v}\beta 6$ -specific mouse monoclonal antibody 10D5 (grey) and the negative control IgG (black) histograms are also shown in each plot. C) Binding to cellular $\alpha\text{v}\beta 6$ by D25 and D34 verified by flow cytometry at 100 (red histogram), 10 (orange histogram) and 1 (green histogram) $\mu\text{g}/\text{ml}$. Size-exclusion chromatography profile of purified of D25scFv and D34scFv showed a major peaks at 30 kDa.
doi:10.1371/journal.pone.0070452.g002

reported is associated with poor survival from cancer, presumed to be because this integrin promotes carcinoma invasion and survival [6–9]. We had identified previously $\alpha\text{v}\beta 6$ -binding peptides from high affinity ligands for $\alpha\text{v}\beta 6$ and shown that interrogation of the peptide structures by various NMR techniques revealed 1) all three ligands (A20FMDV1, LAP, A20FMDV2) were hairpin-shaped peptides with RGD at the turn followed by an helix and 2) the Asp+1 and Asp+4 residues were exposed on the same face of the helix and appeared to form a hydrophobic binding interface with the integrin and 3) potency of $\alpha\text{v}\beta 6$ inhibition appeared to correlate with the length of the helix [14,24]. Thus we designed two algorithms to retain these structural elements while allowing for variation in amino-acid composition and helix length.

We have used our NMR data to design algorithms that would retain the key structural residues that would encode a library of RGD-helix-hairpin structural motifs where the helices would be of varying lengths and sequence composition. We used the algorithms to create two structurally-guided scFv libraries that incorporate either an α - or a 3_{10} -helix C-terminal to the RGD_{LXXL} motif within $V_{\text{H}}\text{-CDR3}$.

Screening of 96 clones isolated following three rounds of biopanning with the combined α -helix and 3_{10} -helix libraries revealed H-CDR3 sequences of both α -type and 3_{10} -type, indicating that both library designs are capable of producing $\alpha\text{v}\beta 6$ -binding scFv. The scFv and the $V_{\text{H}}\text{-CDR3}$ derived peptides from the two lead clones, D25scFv, D34scFv, D25p and D34p: 1) bound only to $\alpha\text{v}\beta 6$ -expressing cells (A375P $\beta 6$) but not to cells that

expressed $\alpha\text{v}\beta 3$, $\alpha\text{v}\beta 5$, $\alpha\text{v}\beta 8$ and $\alpha 5\beta 1$ (A375P_{puro} 2) exhibited dose-dependent inhibition of the $\alpha\text{v}\beta 6$ -specific ligand A20FMDV2 binding to cellular $\alpha\text{v}\beta 6$ 3) inhibited carcinoma cell $\alpha\text{v}\beta 6$ -dependent adhesion to fibronectin 4) and were internalised into cells in an $\alpha\text{v}\beta 6$ -dependent manner. These characteristics make these two lead clones excellent candidates for development as therapeutic antibodies. In advance of this we tested whether the D25p possessed similar *in vivo* targeting capabilities that we had previously shown for A20FMDV2. Data showed that the radiolabelled D25p selectively located to $\alpha\text{v}\beta 6$ -expressing tumours *in vivo* showing that the structurally designed library could generate unique compounds with *in vivo* efficacy and specificity. Our attempts to radiolabel the D25scFv and D34scFv resulted in loss of antibody activity so *in vivo* experiments were not attempted. This will need to be addressed in future studies where radiolabeling protocols will need to be modified. Hence antibody derivatives such as diabody and intact antibody derivatives of D25 and D34 could be studied further in an *in vivo* setting.

Our data also show that RGD-helix structures with very long helices retain excellent $\alpha\text{v}\beta 6$ -specificity and function-blocking activity. Thus D25p has an α -helix almost 3-fold longer than the parental peptide A20FMDV2. Interestingly, the D25p was a more efficient inhibitor of $\alpha\text{v}\beta 6$ -cellular function than D34p which has a shorter α -helix, whereas there was no difference in binding of D34scFv versus D25scFv to cellular $\alpha\text{v}\beta 6$ (Figure 3E). Thus, while we have not established whether there is an optimal length of α -helix for scFv specificity for $\alpha\text{v}\beta 6$, we have established that

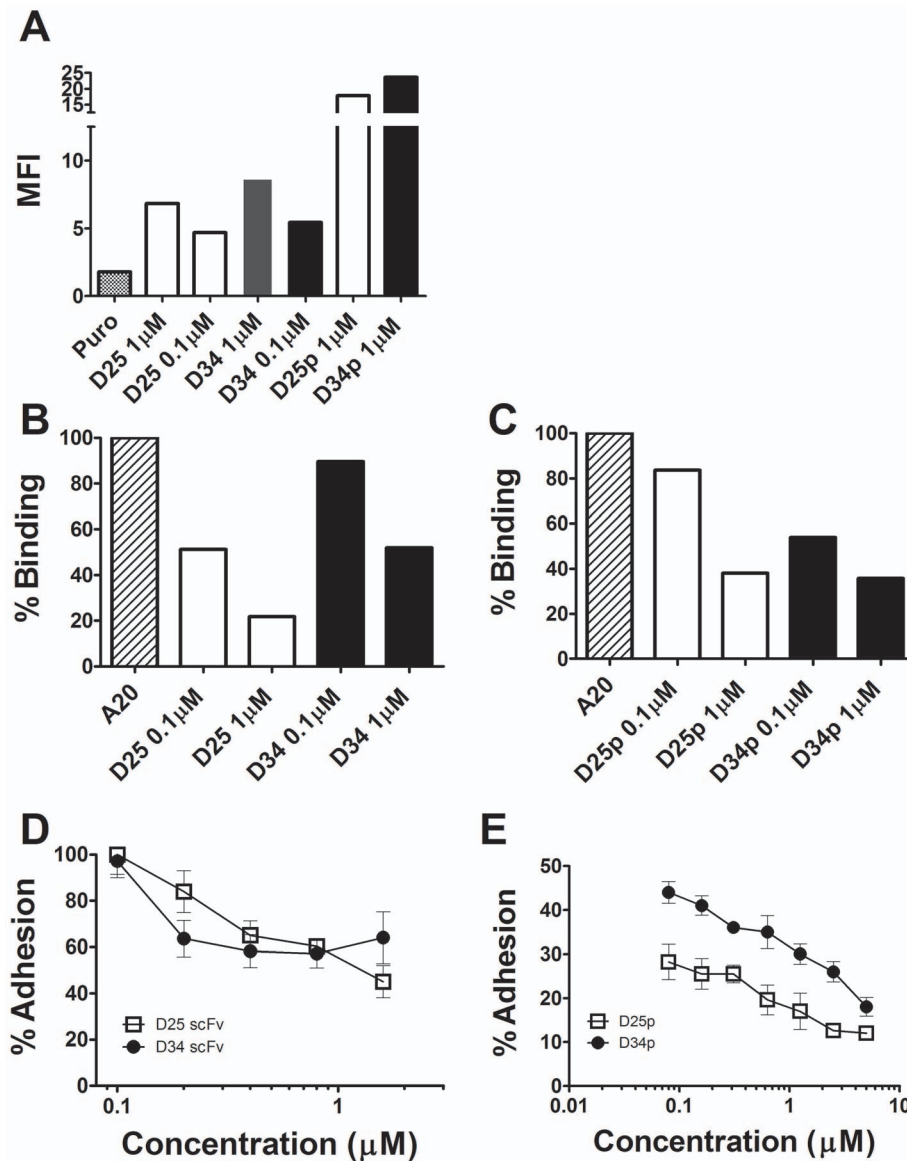


Figure 3. Cellular α ν β 6 binding efficacy of D25scFv, D34scFv, D25p and D34p. A) Binding to A375P β 6 was demonstrated by flow cytometry. The mean fluorescence intensity (MFI) values recorded from representative experiments are shown. A375Puro cells were used for the negative control (puro) where none of the D25scFv or D34 scFvs (data not shown) or peptide derivatives (Figure S1) showed any binding. To avoid repetition in the figure, the bar indicated as puro represent the binding of D25 scFv, D34 scFv which gave similar MFI when the primary scFv or peptide were omitted as the binding to puro control cells (data not shown). B) Dose-dependent inhibition of the α ν β 6 specific binding of A20FMDV2 (A20) was demonstrated with both D25 (D25scFv) and D34 (D34scFv). A20FMDV2 binding is expressed here as a percentage of the MFI value detected in the absence of scFv. C) Dose-dependent inhibition of the α ν β 6 specific binding of A20FMDV2 (A20) was demonstrated with D25p and D34p peptides. A20FMDV2 binding is expressed here as a percentage of the MFI value detected in the absence of peptide inhibitors. D) α ν β 6-dependent adhesion to fibronectin was similarly inhibited by D25scFv and D34scFv ($p > 0.05$). E) α ν β 6-dependent adhesion to fibronectin was inhibited by D25p and D34p. Significantly better inhibition of α ν β 6-dependent adhesion to fibronectin was seen by D25p in comparison to D34p ($p = 0.0156$). doi:10.1371/journal.pone.0070452.g003

relatively large 3D-motif-encoding sequences can be grafted into CDR loops and result in function-blocking antibodies and V_H-CDR3 based peptides.

The concept introduced here can be adopted for other therapeutic targets. Current studies have identified tumour associated receptor tyrosine kinases that are being considered as potential therapeutic targets [25–27] and it is likely that key chemokine receptors [28] also will be similarly targeted. A similar strategy to that described here, using the 3-dimensional shape of the ligand-binding interface for these receptors, can generate

receptor-selective structurally-guided scFv, peptide or any other protein scaffold libraries that would herald a new method for creating valuable therapeutic antibodies. This approach has the potential to replace the traditional approach whereby random libraries are used to develop ligand antagonists and may result in more powerful therapeutic antibodies.

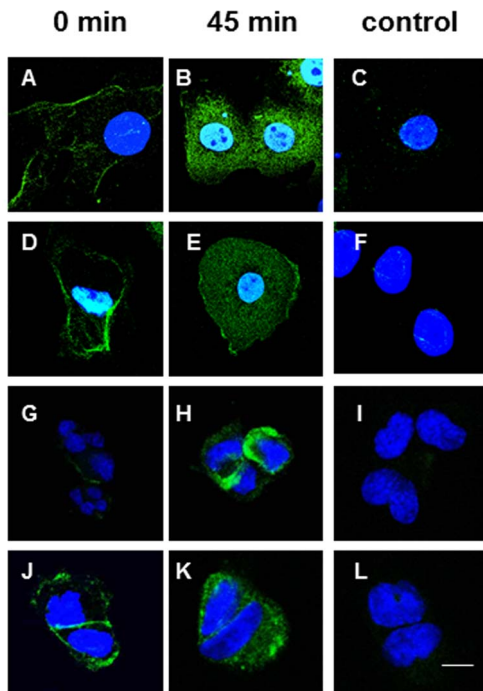


Figure 4. Internalisation of D25scFv, D34scFv, D25p and D34p in $\alpha v \beta 6$ -expressing cells. Internalisation of bound D25scFv (A,B) and D34scFv (D, E) was assessed at 0 mins (A,D) and 45 mins (B,C,E,F) in $\alpha v \beta 6$ -expressing cells (A,B,D,E) and detected using anti-myc antibody. In control cells (C,F) only anti-myc antibody was used. The scFvs both were internalised by $\alpha v \beta 6$ -expressing cells and some located to the nucleus. The absence of nuclear staining with anti-myc antibody alone suggests this was a true nuclear localisation. Internalisation of D25p (G, H, I) and D34p (J, K, L) was assessed in $\alpha v \beta 6$ -expressing cells ((G,H,J,K) and $\alpha v \beta 6$ -negative cells (I, L) at the times indicated. Both peptides were internalised only by $\alpha v \beta 6$ -expressing cells. The scale bar shown represents 20 μm .

doi:10.1371/journal.pone.0070452.g004

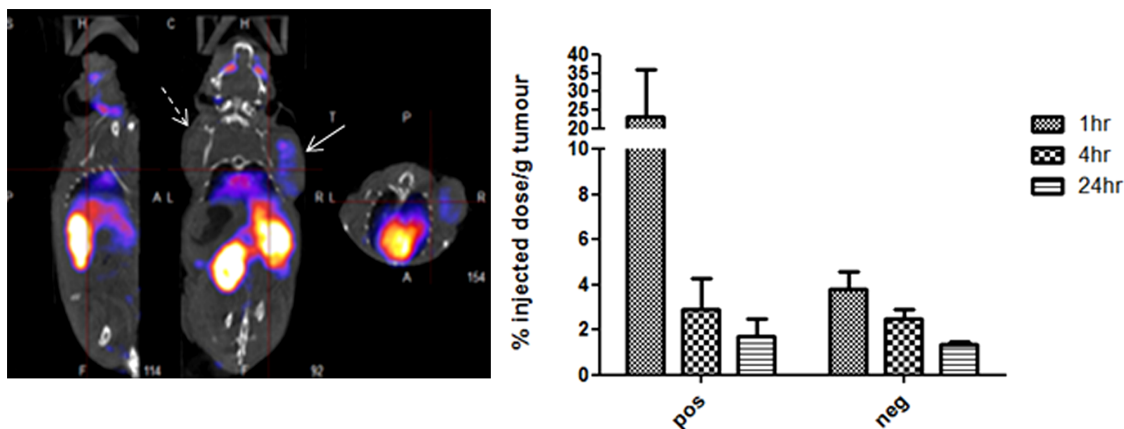


Figure 5. Localization of radiolabelled D25p *in vivo*. Single Photon Emission Computed Tomography imaging was used to localize the Indium-111 radiolabelled D25p *in vivo*. The figure in the left panel represents a representative mouse at the one-hour time point, post injection. The three images represent three different viewing angles – the sagittal (left), coronal (middle) and axial (right). Significantly more radioactivity was retained by the $\alpha v \beta 6$ positive tumour (indicated with solid arrow) compared with the $\alpha v \beta 6$ negative tumour (indicated with the dashed arrow). Quantitative data showing the average retention of radioactivity per gram of tumour in the three tested mice at the 1 h, 4 h and 24 h time points are shown in the histogram. Significantly more radioactivity was retained by the $\alpha v \beta 6$ positive tumour ($p < 0.01$) compared with the $\alpha v \beta 6$ negative tumour, and significantly higher at 1 hr compare to 4 and 24 hr ($p < 0.01$). No significant difference were seen in radioactivity retention in the $\alpha v \beta 6$ negative tumour between 1 hr and 4 and 24 hr in the ($p > 0.05$).

doi:10.1371/journal.pone.0070452.g005

Materials and Methods

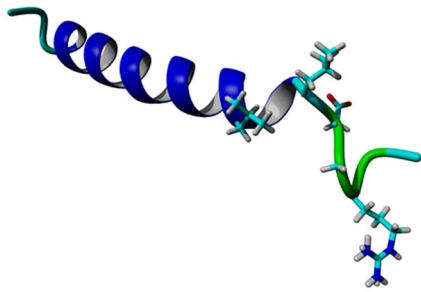
Library construction and selection

Library construction is shown in Figure 7. A pool of 50 human V_H genes cloned into the pHEN1 vector was used as a PCR template [5]. The library initially was amplified with LMB3 primer (Table 1), which anneals to pHEN1 vector sequences 5' to the cloned V_H gene and primer 1 or 2, which anneals to 3' end of the V_H gene which was composed of the frame work 3 (FR3) region, the structurally guided motifs encoded by the α - or 3_{10} -helix algorithms and finally the JH4 sequences (Table 1, Fig. 7A). In a second PCR step, XhoI restriction site was introduced 3' to the JH4 sequence after amplification with primer 1 or 2 and LMB3 (Figure 7B). The V_H gene amplicons containing inserts encoding the algorithms were then digested with XhoI and NcoI restriction enzymes and inserted into the NcoI and XhoI treated pIT2 vector containing the VL repertoire (Fig. 7C, [3]).

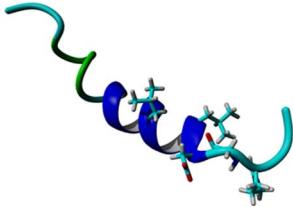
The α -helix and 3_{10} libraries were each rescued separately KM13 helper phage as described previously [29]. For selection, we used in parallel each library separately as well as mixed alpha helix and 3_{10} libraries. The initial phage selection was performed using immobilised recombinant $\alpha v \beta 6$ protein as described previously [5,29] and <http://www.lifesciences.sourcebioscience.com/media/143421/tomlinsonij.pdf>. After two rounds of selection on immobilised $\alpha v \beta 6$ we then selected the libraries on cell-expressed $\alpha v \beta 6$ using A375P $\beta 6$ and A375PPuro cell lines, for $\alpha v \beta 6$ -positive and $\alpha v \beta 6$ -negative selection, respectively [14,22]. First line screening were done by ELISA using 5 $\mu g/ml$ immobilised recombinant $\alpha v \beta 6$ as described [29].

Cell lines

The adherent melanoma cell lines A375P $\beta 6$ and A375PPuro, described previously [22] were cultured in Dulbecco's Modified Eagles' Medium (DMEM) supplemented with 10% Foetal Calf Serum (FCS). The human oral squamous cell carcinoma VB6, which was engineered to express high levels of $\alpha v \beta 6$, was grown in Keratinocyte Growth Medium as described [7].



A. D25p: EPRGDLRTLAAREKRNFNETLARLQEKGI



B. D34p: QPRGDLRELAARSEAQLQEKGI

Figure 6. NMR solution Structure of D25p and D34p. Figure shows the 3D-rendering model for each peptide based on the mean of 20 NMR structures. Both peptides exhibited the RGD-helix motif. D34 which has 22 amino-acids has a shorter helix than peptide D25, which has 29 amino-acids. Helices for both peptides were defined as standard α -helix with the D34 α -helix running from Leu6-Leu17 and D25 α -helix running from Leu6-Gln25.

doi:10.1371/journal.pone.0070452.g006

Screening for integrin specificity by Flow Cytometry

Purified scFv were tested for specificity for $\alpha v \beta 6$ by flow cytometry using the isogenic pairs of cell lines, A375P $\beta 6$ and A375Ppuro, or DX3 $\beta 6$ and DX3puro. Each pair expresses similar levels of four RGD-binding integrins ($\alpha v \beta 3$, $\alpha v \beta 5$, $\alpha v \beta 8$, $\alpha 5 \beta 1$) but only A375P $\beta 6$ and DX3 $\beta 6$ express $\alpha v \beta 6$ [14,22,30]. Briefly, cells were detached with trypsin/EDTA, rinsed twice in ice-cold wash buffer (0.1% BSA/DMEM/0.1% NaN₃) and approximately 2×10^5 cells re-suspended in 50 μ l of wash buffer per sample. In between all incubation steps, all samples were washed twice with wash buffer unless otherwise stated. Cells were incubated on ice for 1 hr with 0.1 or 1 μ M purified scFv of peptide, washed twice. For scFv, cells were then incubated for 1 hr on ice with mouse anti-Myc antibody (clone 9E10, Santa Cruz) at 1:100. After washing, bound antibody was detected with anti-mouse IgG-Alexafluor 488 (1:250 for 1 h; Molecular Probes), on ice. Bound V_H-CDR3 derived peptide were detected by rabbit anti-biotin IgG (1:200), followed by anti-rabbit IgG-Alexafluor 488 (1:250; Molecular Probes). Cells were analysed using the FACSCalibur (Beckton Dickinson). Cell expression of $\alpha v \beta 6$ integrin was detected with mouse monoclonal antibody (clone 10D5, 10 μ g/ml; Millipore) and non-specific (control) binding with non-immune class matched IgG.

Inhibition of $\alpha v \beta 6$ ligand binding

The scFv lead candidates propensity to inhibit binding of the $\alpha v \beta 6$ -specific biotinylated-A20FMDV2 [19] to $\alpha v \beta 6$ -expressing cells was determined by pre-incubation with purified scFv or peptide (0.1 and 1.0 μ M) for 10 mins, immediately followed by 40 mins incubation with the biotinylated A20FMDV2 (10 nM).

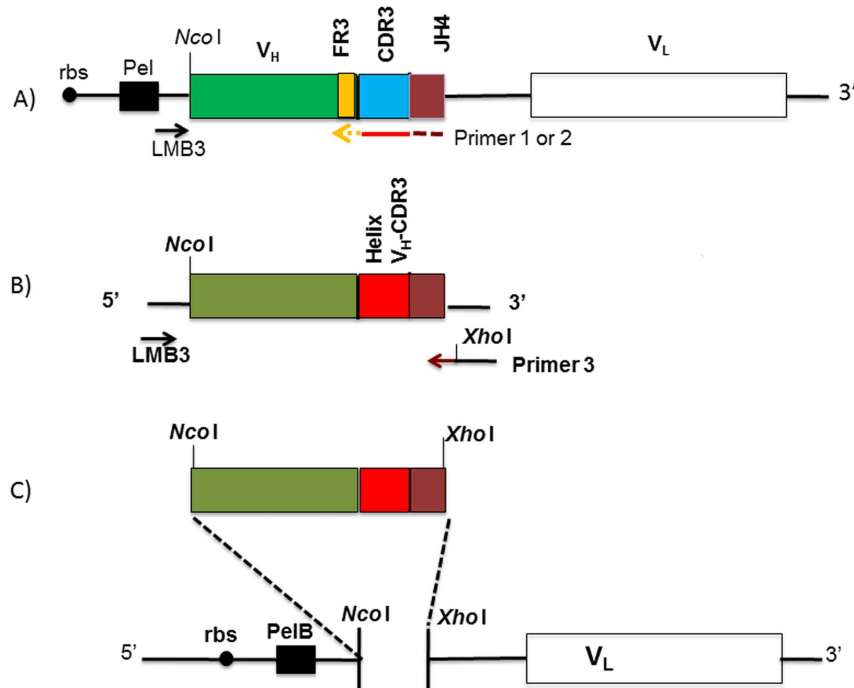


Figure 7. Cloning strategy used to build the scFv phage display libraries with synthetic structurally shaped V_H-CDR3 containing the α - and 3_{10} -helix. A. pHEN1 plasmid backbone containing scFv was used as the PCR template gene to be amplified with the primers LMB3 and the Primer 1 or 2 that includes the FR3 sequences (yellow), flanked by the α - or 3_{10} -helix algorithms (red) and followed by JH4 sequences (brown). B. After PCR amplification the resulted V_H gene segment was rearranged with α - or 3_{10} -helix V_H-CDR3 (red). To incorporate a unique Xho1 restriction site, the PCR products derived from step A were amplified with LMB3 and Primer 3. C. The resultant PCR products from step B were digested with Nco1 and Xho1 for insertion into the pIT2 plasmid backbone that contain light chain repertoire.

doi:10.1371/journal.pone.0070452.g007

Table 1. Oligonucleotides used to build the structural guided library.

Primer I.D	Sequence (5' to 3')
LMB3	CAGGAAACAGCTATGAC
Primer 1/ α -helix	CCAGATCCCTTTCTCTGCAAMNNGGCTAGMNNCTCGTTGAAMNNCCGCTTMNNTCGGGCTGCGAGMNNMNTAGGT- CTCCTCGAGGTTCTCTTGACAGTAATACACGGCCGTGTC
Primer 2/ β -helix	CCAGATCCCTTTCTCTGCAAMNNGGCTAGMNNCTCGTTGAAMNNCCGCTTMNNTCGGGCTGCGAGMNNMNTAGGTCTCCTCGAGGTTCT- TTGACAGTAATACACGGCCGTGTC
Primer 3	GCCTGAACCGCTCCACCACTCGAGACGGTGACCAGGGTACCTTGCC-CCAGATCCCTTTCTCTGCAA
Fdseq	GAATTTTCTGTATGAGG

doi:10.1371/journal.pone.0070452.t001

Bound A20FMDV2 peptides were detected by rabbit anti-biotin IgG (1:200), followed by anti-rabbit IgG-Alexafluor 488 (1:250; Molecular Probes).

Fast protein liquid chromatography (FPLC)

The structural stability of scFv proteins was assessed by gel filtration chromatography using a HiPrep 16/60 sephacryl S-200 (GE healthcare, Amersham, UK) connected to an AKTA FPLC (GE healthcare, Amersham, UK). Fractionations were performed in PBS at a flow rate of 0.3 ml/min with detection at 280 nm. A Calibration Kit (GE healthcare, Amersham, UK) containing protein markers (aprotinin, ribonuclease A, carbonic anhydrase, ovalbumin and conalbumin) was used to generate a calibration curve. Equal amounts of each of the protein markers were prepared to 500 μ l in PBS prior to loading onto the column. Kav values derived from the equation: $K_{av} = (V_e - V_0) / (V_c - V_0)$; where V_e = elution volume, V_c = geometric column volume, and V_0 = column void volume were plotted against log molecular weight to generate a protein calibration curve. Purified scFv (50 μ g/500 μ l) was loaded onto the gel filtration column and molecular weight of the different peaks was determined using the calibration curve.

Internalisation Assay

In 24-well culture plates, 2×10^4 cells α v β 6-positive and -negative cells were seeded onto 13 mm diameter glass coverslips and allowed to incubate overnight at 37°C in growth medium. Cells were washed twice in serum free medium (SFM) and then scFv (4 μ M) or biotinylated-CDR3-peptide (100 nM) diluted in SFM added on ice for 10 mins. After two ice-cold washes and a further 10' on ice with mouse anti-biotin antibody (10 μ g/ml) pre-warmed media containing 10% FCS was added to the cells and incubated at 37°C. At 10 min intervals between 0–60 mins, cells were fixed in 2% HCHO in PBS and permeabilised with 0.1% TritonX-100 (PBS) for 3 mins. scFv was detected with mouse anti c-myc (1:100 dilution, clone 9E10; 30', ambient temperature) while peptides were detected by rabbit anti-biotin IgG (1:200). Both peptide and scFv detected with anti-mouse Alexa488 for 30'. Nuclei were counter-labelled with 4',6-diamidino-2-phenylindole (DAPI), coverslips mounted with Mowiol and samples examined by confocal microscopy (Zeiss LSM510, Welwyn Garden City).

Picogreen adhesion assay

All adhesion assays were performed in quadruplicate and repeated at least 2–3 times. In a 96-well plate format, test wells were coated with Fibronectin (10 μ g/ml/PBS) and negative control wells were coated with 0.1% BSA (bovine serum albumin)/PBS. After incubation at 37°C for 1 hour, plates were washed in PBS twice and blocked with 0.1% BSA/PBS for

30 mins at 37°C. Following a PBS rinse, cells were seeded into the wells, the plate resting on ice to avoid dehydration and to ensure an initial uniform temperature for the experiment. Purified scFv or peptide was added (25 μ l) to the wells at the desired concentrations, before adding 1.5×10^4 cells (25 μ l) per well. In some experiments, cells (1.5×10^4) were pre-treated with β 1 blocking antibody AIB2 at 10 μ g/ml before seeding into test wells to block the β 1-dependent fibronectin adhesion. To determine percentage adhesion, standard curves were generated by plating $0-2.5 \times 10^4$ cells in separate wells. After incubating plates at 37°C for 30' plates were washed twice in 1 mM CaCl_2 /0.5 mM MgCl_2 /PBS and transferred into -80°C for 15 mins. Adherent cells were quantified using a Picogreen kit (Invitrogen) and analysed on a fluorescence reader (FLUOstar Optima, BMG Labtech Ltd, Bucks, UK).

In vivo localization

All animal procedures followed strict Home Office (UK) guidelines under license number PPL 80/2279. Biotinylated-peptide was radiolabelled with Indium-111. To 10 μ g of DOTA-Biotin (Macrocytics.com #C-100) buffered in 1M Ammonium Acetate (pH 5.5) was added Indium [^{111}In]-acetate. The mixture was heated to 80°C for 30 mins and cooled at RT for 10 mins. The labelled DOTA-Biotin was added to streptavidin at a 1:1 Molar Ratio (1 mg of streptavidin per 17.6 μ g of DOTA-Biotin). To this mixture, 88 μ g of biotinylated-D25p was added and 10 μ l of the mixture analysed by size exclusion-HPLC to verify the stability of radiolabelled products pre- and post-labelling (data not shown). A total of 50MBq was used to label 25 μ g of peptide; the sample was divided into four such that each mouse received 12.5 MBq (6.25 μ g) of ^{111}In -labelled D25 peptide.

Female CD1 nu/nu athymic nude mice (Charles River) were subcutaneously injected with 100 μ l (2×10^6 cells) of A373P β 6 into the right shoulder and A375puro in the left shoulder. Tumours were allowed to develop for 20 days and 200 μ l of freshly radiolabelled ^{111}In -labelled D25 peptide was administered intravenously. Tumours were imaged by NanoSPECT/CT (Bioscan, Inc) at 1 hr, 4 hr and 24 hr-time points as follows: Mice were placed onto the imaging bed and initial low resolution CT scans were collected at 45KVp, 180 projections per rotation, 500 ms per projection. Subsequently SPECT images were acquired (45 minutes acquisition time) and data reconstructed using on-board HisPECT-NG software (Bioscan). To measure radioactivity associated with tumours the NanoSPECT/CT machine was calibrated (before the experiment) by imaging a phantom with an Indium-111 standard solution. Subsequently Invivoscope software (Invivo) was used to generate three-dimensional regions of Interest (ROI) around the tumours and the ROIs converted to megabequerels.

Structural determination by NMR study

Solution NMR structures of peptides D25p and D34p on 0.1% TFE were solved as previously [13]. All NMR data for peptides A22 (D25p) and A29 (D34p) were obtained at 283 K from a 14.1 T (600 MHz ^1H) Bruker Avance III NMR spectrometer equipped with a 5 mm QCI-F cryoprobe. All NMR samples were 350 μL within a Shigemi NMR tube and contained 1 mM peptide in 25 mM sodium phosphate buffer at pH 6.5 also containing 50 mM sodium chloride, 4% (v/v) dimethylsulfoxide (DMSO), and 30% (v/v) trifluoroethanol-d3 (TFE). NMR data processing was completed using TopSpin 3.1 (Bruker), assignments were completed using CCPN Analysis.

^1H chemical shifts and through-space structural assignments were obtained from two-dimensional TOCSY and NOESY NMR experiments with mixing times of 20 ms/60 ms for TOCSY and 250 ms for NOESY. The observed NOE contacts support the presence of an α -helical conformation along the length of the peptide with NOEs observed between $\text{H}\alpha$ and HN ($i-i+3$) as well as $\text{H}\alpha$ and $\text{H}\beta$ ($i-i+3$). Structural ensembles were calculated using CNS [31] and including dihedral angles confirmed by DANGLE analysis [31] and predicted hydrogen-bond donor acceptor pairs. The final ensemble was water-minimised using YASARA Structure software (available from <http://www.yasara.org>) and Ramachandran analysis of each peptide ensemble was completed using PROCHECK-NMR [32].

Statistical analysis

The Wilcoxon matched-pairs signed rank test was used to compare activity. Statistical analysis was performed using the GraphPad Prism software package (GraphPad Software, San Diego, CA).

Supporting Information

Figure S1 A375Ppuro cells were incubated with biotinylated D25p or D34p at 1 μM . Bound peptide was detected with rabbit anti-biotin IgG (1:200), followed by anti-rabbit IgG-Alexafluor 488 (1:250; Molecular Probes). Note that there was no significant

References

- Nelson AL, Dhimolea E, Reichert JM (2010) Development trends for human monoclonal antibody therapeutics. *Nat Rev Drug Discov* 9: 767–774.
- Nissim A, Chernajovsky Y (2008) Historical development of monoclonal antibody therapeutics. *Handb Exp Pharmacol*: 3–18.
- de Wildt RM, Mundy CR, Gorick BD, Tomlinson IM (2000) Antibody arrays for high-throughput screening of antibody-antigen interactions. *Nat Biotechnol* 18: 989–994.
- Hanes J, Schaffitzel C, Knappik A, Pluckthun A (2000) Picomolar affinity antibodies from a fully synthetic naive library selected and evolved by ribosome display. *Nat Biotechnol* 18: 1287–1292.
- Nissim A, Hoogenboom HR, Tomlinson IM, Flynn G, Midgley C, et al. (1994) Antibody fragments from a 'single pot' phage display library as immunochemical reagents. *EMBO J* 13: 692–698.
- Nystrom ML, McCulloch D, Weinreb PH, Violette SM, Speight PM, et al. (2006) Cyclooxygenase-2 inhibition suppresses alphavbeta6 integrin-dependent oral squamous carcinoma invasion. *Cancer Res* 66: 10833–10842.
- Thomas GJ, Lewis MP, Hart IR, Marshall JF, Speight PM (2001) AlphaVbeta6 integrin promotes invasion of squamous carcinoma cells through up-regulation of matrix metalloproteinase-9. *Int J Cancer* 92: 641–650.
- Thomas GJ, Lewis MP, Whawell SA, Russell A, Sheppard D, et al. (2001) Expression of the alphavbeta6 integrin promotes migration and invasion in squamous carcinoma cells. *J Invest Dermatol* 117: 67–73.
- Thomas GJ, Nystrom ML, Marshall JF (2006) Alphavbeta6 integrin in wound healing and cancer of the oral cavity. *J Oral Pathol Med* 35: 1–10.
- Van Aarsen LA, Leone DR, Ho S, Dolinski BM, McCoon PE, et al. (2008) Antibody-mediated blockade of integrin alpha v beta 6 inhibits tumor progression in vivo by a transforming growth factor-beta-regulated mechanism. *Cancer Res* 68: 561–570.
- Bates RC, Bellovin DI, Brown C, Maynard E, Wu B, et al. (2005) Transcriptional activation of integrin beta6 during the epithelial-mesenchymal

transition defines a novel prognostic indicator of aggressive colon carcinoma. *J Clin Invest* 115: 339–347.

Figure S2 Structures of RGD peptides D34p (A+B) and D25p (C+D) in 30% w/v TFE. RGD residues are shown as sticks in A and C. Helices are drawn for and ensembles are fitted to residues 6–17 and 6–25 for peptide D34p and D25p respectively. (TIF)

Figure S3 NOE contacts, chemical shift difference, hydrogen bond donors and Dihedral restraints for D34p peptide with 30% w/v TFE. The secondary structure shown beneath the restraints indicates the limits of helix formation according to Ramachandran analysis of the final 20 structure ensemble. (TIF)

Figure S4 NOE contacts, chemical shift difference, hydrogen bond donors and Dihedral restraints for D29p peptide in 30% w/v TFE. The secondary structure shown beneath the restraints indicates the limits of helix formation according to Ramachandran analysis of the final 20 structure ensemble. (TIF)

Table S1 NMR and refinement statistics for 20 structure ensembles of peptides. (DOCX)

Acknowledgments

We thank Dr Jane Sosabowski and Jerome Burnet for their specialist skills in our radio-imaging studies

Author Contributions

Conceived and designed the experiments: AN JM MH YKSM DD NC. Performed the experiments: YKSM DD NC. Analyzed the data: AN JM MH. Contributed reagents/materials/analysis tools: SV SM MR. Wrote the paper: AN JM MH YKSM. Jointly supervised the study: JM AN.

- transition defines a novel prognostic indicator of aggressive colon carcinoma. *J Clin Invest* 115: 339–347.
- Elayadi AN, Samli KN, Prudkin L, Liu YH, Bian A, et al. (2007) A peptide selected by biopanning identifies the integrin alphavbeta6 as a prognostic biomarker for non-small cell lung cancer. *Cancer Res* 67: 5889–5895.
- Hazelbag S, Kenter GG, Gorter A, Dreef EJ, Koopman LA, et al. (2007) Overexpression of the alpha v beta 6 integrin in cervical squamous cell carcinoma is a prognostic factor for decreased survival. *J Pathol* 212: 316–324.
- DiCara D, Rapisarda C, Sutcliffe JL, Violette SM, Weinreb PH, et al. (2007) Structure-function analysis of Arg-Gly-Asp helix motifs in alpha v beta 6 integrin ligands. *J Biol Chem* 282: 9657–9665.
- Kraft S, Diefenbach B, Mehta R, Jonczyk A, Luckenbach GA, et al. (1999) Definition of an unexpected ligand recognition motif for alphav beta6 integrin. *J Biol Chem* 274: 1979–1985.
- Clarke ND, Kissinger CR, Desjarlais J, Gilliland GL, Pabo CO (1994) Structural studies of the engrailed homeodomain. *Protein Sci* 3: 1779–1787.
- Gianni S, Guydosh NR, Khan F, Caldas TD, Mayor U, et al. (2003) Unifying features in protein-folding mechanisms. *Proc Natl Acad Sci U S A* 100: 13286–13291.
- Creighton TE (1992) *Proteins: Structure and Molecular Properties*.
- Saha A, Ellison D, Thomas GJ, Vallath S, Mather SJ, et al. (2010) High-resolution in vivo imaging of breast cancer by targeting the pro-invasive integrin alphavbeta6. *J Pathol* 222: 52–63.
- Jones PT, Dear PH, Foote J, Neuberger MS, Winter G (1986) Replacing the complementarity-determining regions in a human antibody with those from a mouse. *Nature* 321: 522–525.
- Barbas CF 3rd, Languino LR, Smith JW (1993) High-affinity self-reactive human antibodies by design and selection: targeting the integrin ligand binding site. *Proc Natl Acad Sci U S A* 90: 10003–10007.

22. Kogelberg H, Tolner B, Thomas GJ, Di Cara D, Minogue S, et al. (2008) Engineering a single-chain Fv antibody to alpha v beta 6 integrin using the specificity-determining loop of a foot-and-mouth disease virus. *J Mol Biol* 382: 385–401.
23. Hattori T, Umetsu M, Nakanishi T, Togashi T, Yokoo N, et al. (2010) High affinity anti-inorganic material antibody generation by integrating graft and evolution technologies: potential of antibodies as biointerface molecules. *J Biol Chem* 285: 7784–7793.
24. Dicara D, Burman A, Clark S, Berryman S, Howard MJ, et al. (2008) Foot-and-mouth disease virus forms a highly stable, EDTA-resistant complex with its principal receptor, integrin alphavbeta6: implications for infectiousness. *J Virol* 82: 1537–1546.
25. Egloff AM, Grandis JR (2008) Targeting epidermal growth factor receptor and SRC pathways in head and neck cancer. *Semin Oncol* 35: 286–297.
26. Jiang P, Hu Q, Ito M, Meyer S, Waltz S, et al. (2010) Key roles for MED1 LxxLL motifs in pubertal mammary gland development and luminal-cell differentiation. *Proc Natl Acad Sci U S A* 107: 6765–6770.
27. Jung KH, Park BH, Hong SS (2012) Progress in cancer therapy targeting c-Met signaling pathway. *Arch Pharm Res* 35: 595–604.
28. Wang L, Huang T, Chen W, Gao X, Zhou T, et al. (2012) Silencing of CXCR4 by RNA interference inhibits cell growth and metastasis in human renal cancer cells. *Oncol Rep* 28: 2043–2048.
29. Harrison JL, Williams SC, Winter G, Nissim A (1996) Screening of phage antibody libraries. *Methods Enzymol* 267: 83–109.
30. Hausner SH, DiCara D, Marik J, Marshall JF, Sutcliffe JL (2007) Use of a peptide derived from foot-and-mouth disease virus for the noninvasive imaging of human cancer: generation and evaluation of 4-[¹⁸F]fluorobenzoyl A20FMDV2 for in vivo imaging of integrin alphavbeta6 expression with positron emission tomography. *Cancer Res* 67: 7833–7840.
31. Brunger AT, Adams PD, Clore GM, DeLano WL, Gros P, et al. (1998) Crystallography & NMR system: A new software suite for macromolecular structure determination. *Acta Crystallogr D Biol Crystallogr* 54: 905–921.
32. Cheung MS, Maguire ML, Stevens TJ, Broadhurst RW (2010) DANGLE: A Bayesian inferential method for predicting protein backbone dihedral angles and secondary structure. *J Magn Reson* 202: 223–233.